Zonal flows and transient dynamics of the L-H transition

Eun-jin Kim and P. H. Diamond

Department of Physics, University of California San Diego, La Jolla, CA 92093-0319

Abstract

We elucidate the role of zonal flows in transient phenomena observed during L-H transition by studying a simple L-H transition model which contains the evolution of zonal flows, mean $\mathbf{E} \times \mathbf{B}$ flows, and the ion pressure gradient. Zonal flows are shown to trigger the L-H transition and cause time-transient behavior through the self-regulation of turbulence before a mean shearing due to a steep pressure profile secures a quiescent H mode. Surprisingly, this self-regulation *lowers* the power threshold for the ultimate transition to a quiescent H-mode state.

The confinement of particles and heat in magnetically confined fusion devices degrades as an input power is ramped up. This is not unexpected since the input power is stored as free energy in background (e.g., density and temperature) profiles, which is then released by various microinstabilities. These microinstabilities cause anomalous transport, thereby degrading confinement. What is surprising is that as an input power is further increased beyond a critical value, plasmas organize themselves into a high confinement state (H mode) by the formation of transport barriers in the plasma edge (or core). This transition from L (low confinement) mode to H mode (the so–called L-H transition) seems to be universal, reproduced in most fusion devices [1] since its first discovery in ASDEX [2]. Since a H mode is an ideal operational regime for future reactors, the detailed study of L-H transition remains as a crucial issue in fusion theory. The importance of a transport barrier is not limited to magnetically confined plasmas, but has also been widely recognized in other systems such as geophysical, atmospheric sciences, etc [3].

One of the most convincing explanation for L-H transition is the suppression of turbulence by $\mathbf{E}\times\mathbf{B}$ flow shearing [4]. This shear suppression can occur by mean $\mathbf{E}\times\mathbf{B}$ flows $\langle V_E \rangle$ and/or by zonal flows $\tilde{V}_E$. While mean $\mathbf{E}\times\mathbf{B}$ flows were initially thought to be responsible for the turbulence suppression, recent studies revealed a crucial role of self generated zonal flows in regulating turbulence [5,6]. Compared to mean $\mathbf{E}\times\mathbf{B}$ flows, zonal flows possess fine spatial structure with a finite, but small, frequency, with their shearing rate being proportional to $\langle (\partial_r \tilde{V}_E)^2 \rangle^{1/2}$ [7]. Because of their small spatial structure, the shearing due to zonal flows is likely to dominate that due to mean flow before the amplitude of the mean flow becomes sufficiently large due to profile steepening (i.e., before and during the L-H transition). Note that zonal flows are excited solely by fluctuation-driven Reynolds stress, while mean $\mathbf{E}\times\mathbf{B}$ flows are driven by mean pressure gradient and poloidal and toroidal flows, which can be generated by external sources, as well as by fluctuations, etc. Thus, mean and zonal flows are likely to play quite different roles in the L-H transition.

In this Letter, we study the role of zonal flows and transient dynamics of the L-H transition. To this end, we propose a concrete model for the L-H transition, which contains the essential physics of mean flows, zonal flows, and the ion pressure profile, and which treats the interplay between mean and zonal flows. Through this model, we explicitly show that zonal flows (1) trigger the transition by regulating turbulence via shearing and (2) cause the observed time-transient (oscillatory or bursty) behavior before the system evolves into a quiescent H mode due to the build-up of a strong mean shearing. The oscillatory behavior near L-H transition, such as dithering in ASDEX Upgrade [8], IM-mode in DIII-D [10], etc, has been known for some time, stimulating many workers to propose numerous different models. For instance, a limit cycle oscillation between L and H states related to the bifurcation curve structure was proposed in [9], while the self-regulation of a poloidal flow was invoked in [10]. Note that most previous works on this issue envisioned the self-regulation of turbulence as originating from mean poloidal or toroidal flows which are self-generated by Reynolds stress [11]. However, Reynolds stress drive for mean flows is likely to be very weak as compared to that for zonal flows, due to the larger scales of the former. Thus, the self-regulation of turbulence (causing time transience) is more likely to occur by zonal flows than by mean flows. The importance of zonal flows in L-H transition was experimentally demonstrated only recently, through bicoherence analysis on DIII-D experimental data [12]. Ref. [12] clearly demonstrated enhanced nonlinear coupling between low and high frequency modes before and during the L-H transition, as well as eventual disappearance of this coupling after the L-H transition when high frequency modes (which drive low frequency modes) are quenched. Note that these low frequency modes are most likely to be zonal flows. Another distinguishing feature of our model is that it treats the interplay between zonal and mean flows, namely the inhibition of zonal flow growth by mean flows (see below), and covers the entire dynamics of L-H transition (from L-mode to quiescent H mode) by the incorporation of a pressure profile evolution, in contrast to Ref. [10].

Before presenting our model, we illustrate the inhibition of zonal flow growth by a mean flow in the case of simple drift wave turbulence. The response of drift wave spectrum $\tilde{N}_k$ to a seed zonal flow $\tilde{V}_E$ of wave number q is given by the following linearized wave kinetic equation

$$\frac{\partial}{\partial t}\tilde{N}_k + iqv_{gx}\tilde{N}_k - k_\theta\langle V_E'\rangle\frac{\partial}{\partial k_r}\tilde{N}_k + \gamma\tilde{N}_k = iqk_\theta\tilde{V}_E\frac{\partial}{\partial k_r}\langle N_k\rangle\,. \tag{1}$$

Here, $N_k = (1+\rho_s^2k^2)^2|\phi_k'|^2$ is the drift wave quanta density; ϕ' is the electric potential of drift waves; γ and $\Delta\omega$ are the linear growth and nonlinear damping rates ($\gamma\langle N_k\rangle = \Delta\omega\langle N_k\rangle^2$), and v_g is the group velocity (in the moving frame with $\mathbf{E}\times\mathbf{B}$ velocity) of drift waves. To explicitly incorporate the effect of $\langle V_E\rangle$ on $\tilde{N}_k$, we define a total time derivative $D_t = \partial_t - k_\theta\langle V_E'\rangle\partial_{k_r}$ and solve Eq. (1) along a non-perturbed, shearing ray orbit from an initial time t_0 to final time t as

$$\tilde{N}_k(q,t) = \int_{t_0}^{t} dt' iqk_\theta\tilde{V}_E(q,t')\frac{\partial\langle N_k(t')\rangle}{\partial k_r(t')}\exp\left\{-\gamma(t-t') - iq\int_{t'}^{t} dt'' v_{gx}(t'')\right\}, \tag{2}$$

where $(t-t_0)\gamma \gg 1$ was used. By realizing that $D_tk_r = -k_\theta\langle V_E'\rangle$, one can easily see that the shearing by a mean flow enters into v_{gx} and $\partial\langle N_k(k_r(t'))\rangle/\partial k_r(t')$. In the limit where the mean shearing occurs on time scale larger than other dynamical time scales (i.e., $1/\gamma$, $1/v_{gx}q$, and $1/\Omega$), we can approximate $\partial\langle N_k(k_r(t'))\rangle/\partial k_r(t') \sim \partial\langle N_k(k_r(t))\rangle/\partial k_r(t)$. Then, the substitution of the time dependence of $\exp\{-i\Omega t\}$ for $\tilde{N}_k$ and $\tilde{V}_E$ simplifies Eq. (2) to

$$\tilde{N}_k(q,\Omega) \sim iqk_\theta\tilde{V}_E R\frac{\partial\langle N_k\rangle}{\partial k_r}\,. \tag{3}$$

Here, the real part of R becomes

$$Re(R) \sim \frac{1}{\gamma}\left[1 - \frac{12q^2\langle V_E'\rangle^2\omega_*^2k_\theta^2}{\gamma^4}\right], \tag{4}$$

for $k_\perp\rho_s < 1$ and $\gamma > qv_{gx} > \Omega$. Here, $\omega = \omega_*/(1+\rho_s^2k^2)$ is used ($\omega_* = k_\theta c_s/L_n$ is the ion drift frequency). Note that the sign of $Re(R)$ is positive since Eq. (4) is derived in the limit of weak mean shear. By coupling Eq. (3) to the evolution equation of zonal flows $-\Omega\tilde{V}_E(q,\Omega)/q = \int d^2k k_\theta k_r\tilde{N}_k(q,\Omega)/(1+\rho_s^2k^2)^2$, we obtain the frequency of zonal flows Ω as

$$\Omega \sim iq^2\int d^2k\frac{k_\theta^2k_r}{(1+\rho_s^2k^2)^2}R\left(-\frac{\partial\langle N_k\rangle}{\partial k_r}\right)\,. \tag{5}$$

Eqs. (4) and (5) clearly demonstrate that *a mean shear flow inhibits the growth of zonal flow.* This inhibition is essentially due to the weakening of the response of drift wave spectrum to a seed zonal flow via the enhanced decorrelation of drift wave propagation by a mean shear flow. This result, obtained in a weak shear limit, will certainly apply to a strong shear case, and thus will be used in the following model for L-H transition.

Our model is based on 0-dimensional (0D) envelop equations, consisting of the amplitudes of turbulence $\mathcal{E}$, zonal flow shear $V_{ZF} \propto \partial_r \tilde{V}_E$, mean flow shear $V \propto \partial_r \langle V_E \rangle$, and the gradient of a (ion) pressure $\mathcal{N} \propto \partial_r p_i$:

$$\partial_t \mathcal{E} = \mathcal{E}\mathcal{N} - a_1 \mathcal{E}^2 - a_2 V^2 \mathcal{E} - a_3 V_{ZF}^2 \mathcal{E} \,, \tag{6}$$

$$\partial_t V_{ZF} = b_1 \frac{\mathcal{E} V_{ZF}}{1 + b_2 V^2} - b_3 V_{ZF} \,, \tag{7}$$

$$\partial_t \mathcal{N} = -c_1 \mathcal{E}\mathcal{N} - c_2 \mathcal{N} + Q \,. \tag{8}$$

Here, a_i, b_i, and c_i are model-dependent constants, whose values may be found in [11]. The exact form of these constants is not pertinent to the qualitative discussion of this Letter and will be given in detail in future publications, as a part of comparison with a specific experimental results. Eq. (6) describes the evolution of turbulence: the first term on the right hand side represents its generation by pressure gradient via linear instability, the second nonlinear saturation of turbulence, and the third and last terms shear suppression of turbulence by mean $\mathbf{E} \times \mathbf{B}$ flows and zonal flows, respectively. Note that $a_2 \simeq a_3$ in the limit where the frequency of zonal flows is much smaller than the decorrelation time of turbulence [13]. The first and second terms on the right hand of Eq. (7) illustrate the generation of V_{ZF} by Reynolds stress and zonal flow damping, respectively. Note that the growth inhibition by a mean shear, which is valid even for a strong shear, is modeled by a term $1/(1 + b_2 V^2)$. The three terms on the right hand side of Eq. (8) represent, from the left, the turbulent diffusion of the pressure profile by turbulence, neoclassical transport, and input power. By assuming a constant ion temperature profile and by ignoring mean toroidal and poloidal flows, for simplicity, the above set of equations is to be closed by the following approximation to the ion momentum balance equation:

$$V = d\mathcal{N}^2 \,. \tag{9}$$

The control parameter of Eqs. (6)–(9) is the input power Q. As the input power Q is increased from below, the mean pressure gradient becomes steeper and excites turbulence. When the turbulent drive becomes sufficiently strong to overcome flow damping, it generates zonal flows by Reynolds stress. Turbulence and zonal flows then form a self-regulating system as the shearing by zonal flows damps the turbulence. A signature of this self-regulation is manifested in time transient (oscillatory or bursty) behavior of the system [6,14,15]. Note that oscillatory behavior can originate from other causes [9]. For a sufficiently high Q, this self-regulation turns off the turbulence, and subsequently zonal flows, are depleted by a mean shearing, and the system evolves into a quiescent H mode

$$\mathcal{E} = V_{ZF} = 0\,, \mathcal{N} = \frac{Q}{c_2}\,. \tag{10}$$

Here, the slope of the profile is determined by neoclassical transport. This quiescent H mode will eventually terminate upon the further increase of gradients when MHD instability sets in. This regime, however, shall not be discussed in the present Letter. What is the effect of mean flows on zonal flows in this scenario? Since the mean flow inhibits the growth of zonal flows, it weakens the damping of turbulence by zonal flows. Therefore, it will prolong the oscillatory phase, leading to a slight increase in the critical input power Q needed to achieve the quiescent state, as compared to the case where this effect is ignored.

The forgoing expectation is now confirmed by the numerical solution of Eqs. (6)–(9). We assume $Q = 1.0 \times 10^{-2} t$ (t is time) and constant values for parameters a_i, b_i, c_i, and d, and study how the system evolves into a quiescent H mode. The results are plotted in Fig. 1 which shows the evolution of $\mathcal{E}$ (solid line), V_{ZF} (dotted line), and $\mathcal{N}/5$ (dashed line). Clearly there are three distinct stages. The early stage is characterized by growing turbulence (by linear instability from increasing $\mathcal{N}$), followed by rapidly growing self-generated zonal flows. As the shearing by zonal flows sufficient to damp turbulence, the system self-regulates, entering into a transition regime, where zonal flows and turbulence compete and exhibit oscillatory behavior: $\mathcal{E}$ and V_{ZF} grow as they draw energy from $\mathcal{N}$ and $\mathcal{E}$, respectively, while $\mathcal{E}$ and $\mathcal{N}$ damp on account of growing V_{ZF} and $\mathcal{E}$, respectively. Notice in Fig. 1 that in addition to oscillation, there is a gradual increase in $\mathcal{E}$. As noted previously, this is due to the reduction in the zonal flow growth by the mean shear flow, which promotes the growth of turbulence. A slight decrease in the amplitude of oscillation is due to nonlinear damping of drift waves ($a_2\mathcal{E}^2$). The behavior of this envelope is given by a stationary solution $\mathcal{E} = b_1(1 + b_2V^2)/b_3$ (see Eq. (7)), which increases as the profile steepens ($V = d\mathcal{N}^2$). The final stage of the evolution (i.e., a quiescent H mode) is marked by the complete damping of turbulence and zonal flows due to strong mean flow shearing for sufficiently large Q. At this stage, the profile steepens linearly with Q, consistent with Eq. (10).

To demonstrate that the inhibition of zonal flow growth by a mean shear flow (term with b_2V^2 in Eq. (7)) prolongs the oscillatory transition phase, we plot the results obtained with $b_2 = 0$ in Fig. 2, using the same parameter values as in Fig. 1. Note that, in this case, the oscillation of $\mathcal{E}$ is about a roughly constant value, in contrast to Fig. 1. This constant value is again given by a stationary solution $\mathcal{E} = b_3/b_1 = 2/3$ with $b_2 = 0$ (see Eq. (7)).

Since zonal flows regulate turbulence before the transition to a quiescent H mode, they trigger the transition by lowering the power threshold, relative to the case without zonal flows. This important effect can clearly be seen in Fig. 3, which represents the evolution of $\mathcal{E}$ (solid) and $\mathcal{N}$ (dashed line) for the same parameters values as in Fig. 1, but with $V_{ZF} = 0$, i.e., the turbulence amplitude is too large to reach a quiescent H mode for the values Q up to 2; the transition will occur at higher value, i.e., $Q > 2$. For comparison, the Q dependence of $\mathcal{E}$ and $\mathcal{N}$ in Fig. 1 are superimposed by dotted and dotted-dashed lines, respectively, in Fig. 3.

A detailed test of the role of zonal flows in L-H transition and identification of the origin of the oscillatory behavior remains as a challenge to experimentalists. First of all, a careful control over the input power ramping is necessary, since the duration of the transition regime sensitively depends on the rate of input power ramping — too rapid ramping shrinks this regime to an arbitrary short time interval, smaller than that of the experimental time resolution. Secondly, the distinction between mean poloidal flows and zonal flows should be made experimentally. A recent experiment on DIII-D [10] successfully resolved a time transient regime (IM mode) by slowly increasing the input power. However, the time transient behavior was interpreted to originate from a self-generated poloidal flow, without a clear identification of the latter. In our model, the zonal flow is the main source of a poloidal flow, in view of the weak Reynolds stress drive for mean poloidal flow. Note that our model provides a concrete route leading to a quiescent H mode by a pressure profile steepening, unlike that of Ref. [10].

In summary, we have proposed and studied a self-consistent 0D model for L-H transition, by incorporating the effect of zonal flows. The uniqueness of this model lies in the synergy of the evolution of zonal flows, mean $\mathbf{E} \times \mathbf{B}$ flows, and mean pressure profile, which permits a qualitative study of the dynamics of the transition deep into quiescent H mode as the input power is ramped up. The key results are (1) that zonal flows trigger the L-H transition, causing time transient behavior, before the system evolves into a quiescent H mode by a steep pressure gradient for a sufficiently large input power, and (2) that mean shear flow, through zonal flow growth inhibition, causes a prolonged duration of the oscillatory transition phase and a slow rise in the envelope of the oscillation. A quantitative comparison with specific experimental data requires the computation of model dependent constants (a_i, b_i, c_i, and d) as well as the relaxation of the assumption of a constant ion mean temperature. Ultimately, it is necessary to extend our model to 1D to study the location and propagation of transport barrier (pedestal). This is particularly interesting since the role of zonal flows in the dynamics of transport barrier is largely unknown. It seems reasonable to hypothesize that the local zonal flow spectral density must be incorporated into barrier dynamics models, along with the local fluctuation intensity. These issues will be discussed in future publications.

Acknowledgments We thank G.R. Tynan and C. Holland for a critical reading of the manuscript. This research was supported by U.S. DOE FG03-88ER 53275.

REFERENCES

[1] DIII-D team, K.H. Burrell et al, Plasma Phys. Controlled Fusion **34**, 1859 (1992).

[2] ASDEX team, F. Wagner et al, Phys. Rev. Lett. **49**, 1408 (1982).

[3] C.R. Or and F.H. Busse, J. Fluid Mech. **174**, 313 (1987); M.E. McIntyre, J. Atmospheric and Terrestrial Phys.**51**, 29 (1989).

[4] K.H. Burrell, Phys. Plasmas **4**, 1499 (1997).

[5] P.H. Diamond, *et al.,* in *Plasma Phys. and Controlled Nuclear Fusion Research* (IAEA, Vienna, 1998) IAEA-CN-69/TH3/1.

[6] Z. Lin, *et al.*, Phys. Rev. Lett. **83**, 3645 (1999); P. Beyer, *et al.*, Phys. Rev. Lett. **85** 4892 (2000); M. Jakubowski, *et al.*, Phys. Rev. Lett. **89**, 265003 (2002); M.G. Shats and W.M. Solomon, Phys. Rev. Lett. **88**, 045001 (2002).

[7] P.H. Diamond, Nuclear Fusion **41**, 1067 (2001).

[8] ASDEX team, H. Zohm *et al.*, Phys. Rev. Lett. **72**, 222 (1994).

[9] S.-I. Itoh, *et al.*, Phys. Rev. Lett. **67**, 2485 (1991).

[10] R.J. Colchin, *et al.*, Phys. Rev. Lett. **88**, 255002 (2002).

[11] P.H. Diamond, *et al*, Phys. Rev. Lett. **72**, 2565 (1994); B.A. Carreras, *et al*, Phys. Plasmas **2**, 2744 (1995).

[12] R.A. Moyer, *et al*, Phys. Rev. Lett. **87**, 135001 (2001); P.H. Diamond, *et al*, Phys. Rev. Lett. **84**, 4842 (2000).

[13] T.S. Hahm, *et al.*, Phys. Plasmas **6**, 922 (1999).

[14] M. Malkov, *et al*, Phys. Plasmas **8**, 5073 (2001); M. Malkov, P.H. Diamond, Phys. Plasmas **8**, 3996 (2001).

[15] E. Mazzucato, *et al.*, Phys. Rev. Lett. **77**, 3145 (1996).

Figure Captions

Fig. 1. Evolution of $\mathcal{E}$ (solid line), V_{ZF} (dotted line), and $\mathcal{N}/5$ (dashed line) as a function of input power $Q = 0.01t$. Parameter values are $a_1 = 0.2$, $a_2 = a_3 = 0.7$, $b_1 = 1.5$, $b_2 = b_3 = 1$, $c_1 = 1$, $c_2 = 0.5$, and $d = 1$.

Fig. 2. The same as Fig. 1 besides $b_2 = 0$.

Fig. 3. Evolution of $\mathcal{E}$ (solid line) and $\mathcal{N}$ (dashed line) as a function of input power $Q = 0.01t$ with $V_{ZF} = 0$. Parameter values are the same as Fig. 1. For comparison, $\mathcal{E}$ (dotted line) and $\mathcal{N}$ (dotted-dashed line) in Fig. 1 are superimposed.

FIGURES

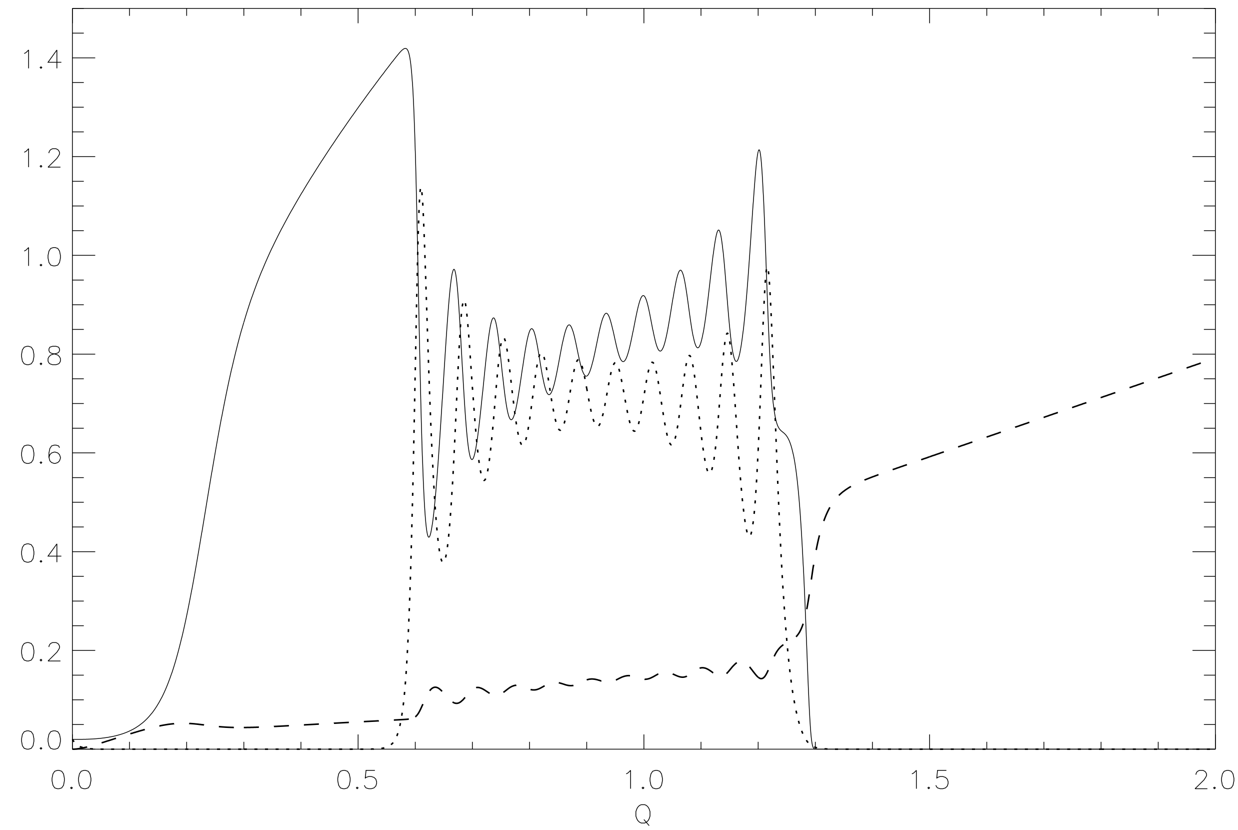

FIG. 1.

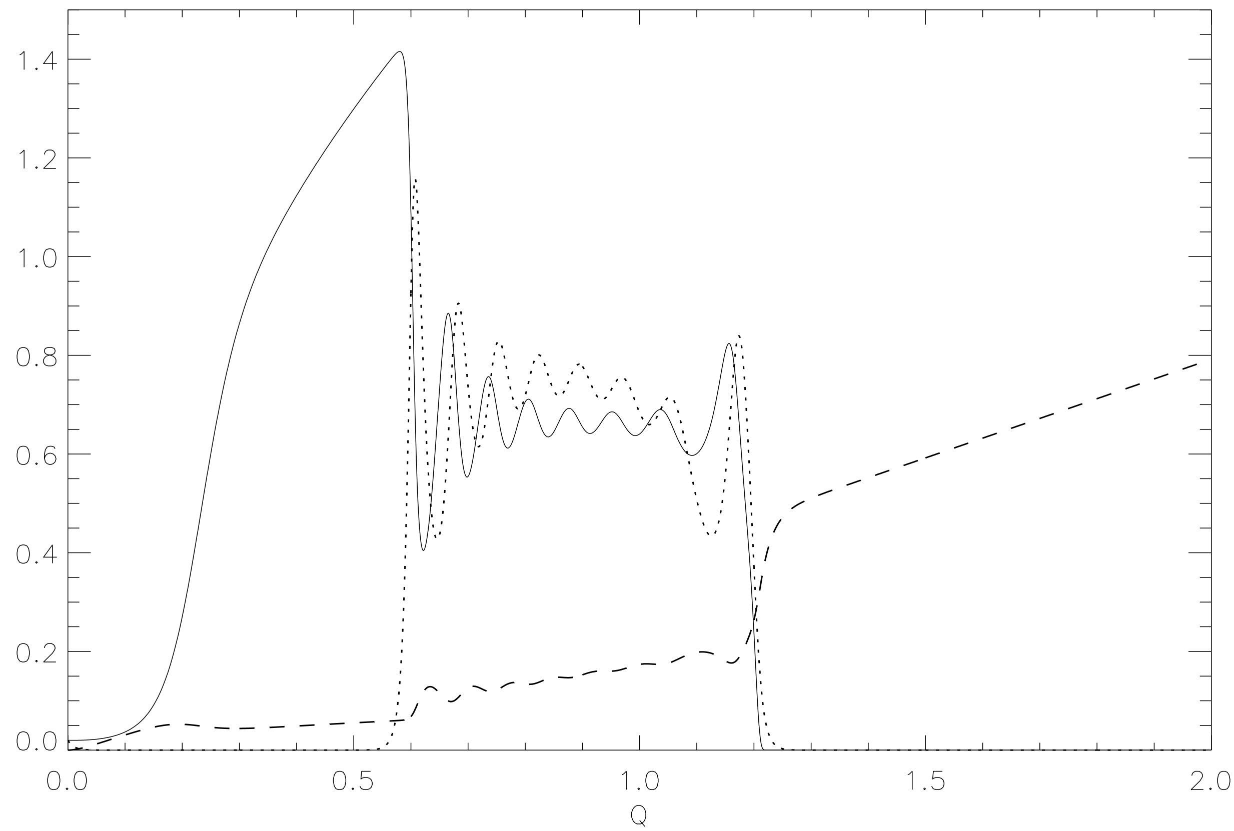

FIG. 2.

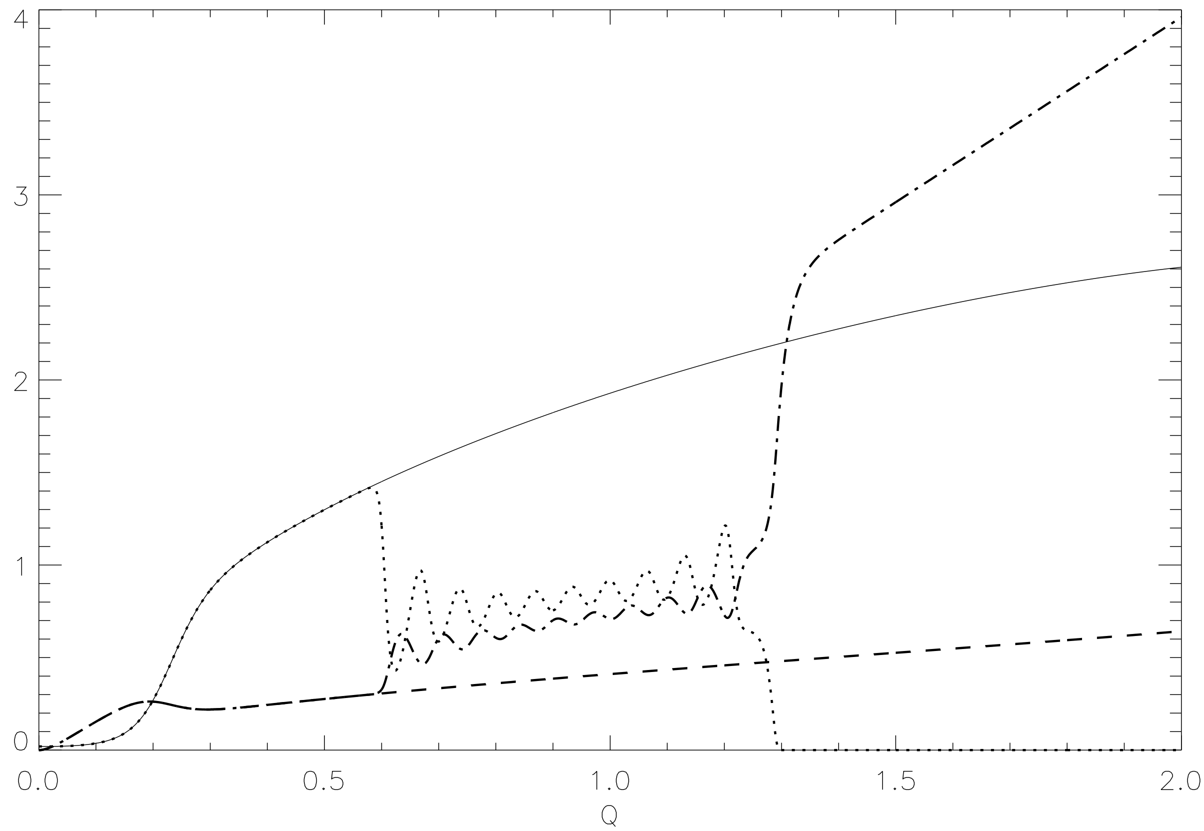

FIG. 3.